



Article

Planning and Analysis of Microgrids for Fast Charging Stations Considering Net Zero Energy Building Indexes

Matheus Souza da Cruz¹, Caroline Beatriz Fucks Darui^{1,2}, Alzenira da Rosa Abaide¹, Nelson Knak Neto^{3,*}, Leonardo Nogueira Fontoura da Silva¹ and Laura Lisiane Callai dos Santos³

¹ Graduate Program in Electrical Engineering, Federal University of Santa Maria, Santa Maria 97105-900, RS, Brazil; matheus.cruz@acad.ufsm.br (M.S.d.C.); caroline@san.uri.br (C.B.F.D.); alzenira@ufsm.br (A.d.R.A.); leonardo.fontoura@acad.ufsm.br (L.N.F.d.S.)

² Electrical Engineering Course, Integrated Regional University, Santo Ângelo 98802-470, RS, Brazil

³ Academic Coordination, Federal University of Santa Maria, Cachoeira do Sul 96503-205, RS, Brazil; laura.santos@ufsm.br

* Correspondence: nelson.knak@ufsm.br

Abstract: Distributed Energy Resources (DERs) aggregation increases the sustainability of the Electric Vehicles (EVs) market. For example, Fast Charging Stations (FCSs) associated with distributed generation and storage systems in a microgrid infrastructure may be beneficial in increasing self-consumption and peak-shaving strategies and mitigating impacts on the grid. However, microgrid sizing planning is a complex challenge, mainly due to numerous factors related to EV market growth and user behavior. This work defines a methodology focusing on sizing planning and analysis of microgrids for FCSs based on quantitative indices formulated according to the Net Zero Energy Building (NZEB) concept, optimizing self-sufficiency and limiting impacts on the primary electrical grid. The methodology is applied to a real case study considering the growth of EVs in southern Brazil. The developed analyses demonstrate that the proposed microgrid meets the energy needs of the FCS and presents the best NZEB indexes within the considered study horizon. Additionally, representative profiles were characterized for different load and generation conditions, complementing the analyses. It was shown that the storage promotes a delay and reduction in the reverse peak power flow, further enhancing the NZEB indexes.

Keywords: microgrids; fast charging stations; net zero energy building; electric vehicles



Citation: da Cruz, M.S.; Darui, C.B.F.; Abaide, A.d.R.; Knak Neto, N.; da Silva, L.N.F.; dos Santos, L.L.C. Planning and Analysis of Microgrids for Fast Charging Stations Considering Net Zero Energy Building Indexes. *Energies* **2024**, *17*, 6488. <https://doi.org/10.3390/en17246488>

Academic Editor: Tek Tjing Lie

Received: 11 November 2024

Revised: 17 December 2024

Accepted: 18 December 2024

Published: 23 December 2024



Copyright: © 2024 by the authors. Licensee MDPI, Basel, Switzerland. This article is an open access article distributed under the terms and conditions of the Creative Commons Attribution (CC BY) license (<https://creativecommons.org/licenses/by/4.0/>).

1. Introduction

In recent decades, growing concerns about the Earth's rising average global temperature have prompted numerous countries to establish goals for reducing their Greenhouse Gas Emission (GEE) indices, with the most recent ones outlined in the Paris Agreement. This Agreement's primary objective was to prevent a 2 °C increase in the Earth's temperature by the end of the 21st century [1]. Among the significant GEE emitters, the transportation sector contributes to 24% of the total global CO₂ emissions, emphasizing the necessity for sectoral decarbonization [2].

In this context, the electrification of the mobility sector emerges as a critical strategy to meet the goals set in international agreements. Electric Vehicles (EVs) utilize different energy source technologies for propulsion, distinguishing themselves by not relying on fossil fuels and emitting no atmospheric pollutants from their exhausts [3]. As a result, many countries, including China, European countries, and the United States, have implemented public policies to promote the development and adoption of EVs, aiming to replace traditional Internal Combustion Engine Vehicles (ICEVs) [4]. Notably, initiatives like EV30@30 have set the goal that 30% of total vehicles sold by 2030 should be EVs in participating countries [5]. Despite being in the early stages of electromobility, Brazil has

the federal program “Rota 2030”, aiming to encourage the automotive sector’s development with a focus on environmental sustainability and citizenship, seeking cost reduction and technological differentiation [6]. This program has led to the creation of incentives, including a reduction in the Industrialized Product Tax (IPI) for pure and hybrid EVs [7].

Despite the incentives implemented in the electrification of the transportation sector, international experience has demonstrated a mutual dependence between the public structure of charging stations and the widespread adoption of EVs. It indicates that the number of FCSs increases with the growing presence of these vehicles on roads, and vice versa. Additionally, several analysts suggest that, among the approximate 10% of recharges conducted at public infrastructures, a significant portion will occur at FCSs located on highways, allowing travel beyond the vehicles’ autonomy with a reduced charging duration time [8,9].

However, the development of FCSs poses challenges related to the high demands imposed by these infrastructures, where a single charger power is higher than 50 kW [10]. An alternative to reduce the power demand of FCSs is to associate locally distributed generation systems—such as photovoltaic (PV) and wind turbines—and energy storage systems to smooth the generation profile [11,12]. In this way, these Distributed Energy Resources (DERs) interconnections compose a microgrid topology, which can operate similarly to the large Electrical System but on a reduced scale [13].

Microgrid operation could reduce energy losses throughout the distribution system and enhance reliability in the local system due to its flexibility in isolating itself from the utility grid during external faults [14]. However, both the intermittency of microgeneration and periods of low demand can negatively impact the primary distribution network’s power quality. Also, since the main load of this type of microgrid is Fast Charging charger units, the sizing and operational planning are influenced by stochastic patterns. On the long-term horizon, these patterns are mainly related to the EV market growth and the technological evolution of EVs. On the other hand, the short-term horizon handles user behaviors, trying to solve when/where and how much energy will be used [15]. Therefore, energy planning must be considered to ensure the operation of these microgrids, as observed in the case of FCSs [16].

In this context, the Net Zero Energy Building (NZEB) concept has garnered worldwide attention from researchers and the industry. This is because it relates to the intelligent and sustainable development of electrical networks [17]. In brief, NZEB is a definition of energy self-sufficiency aiming to optimize the utilization of local Renewable Energy Resources (RERs) in a building, generating as much energy as consumed over a period, approaching a net-zero balance [18]. In the case of microgrids, NZEB can aid in energy planning by making them as independent as possible, maximizing self-sufficiency while minimizing impacts on the primary distribution network [19].

Other reasons supporting adopting the NZEB concept include changes in how these functionalities interact with the grid, characterized by Energy Communities and Local Markets, for example. Additionally, in the Brazilian context, changes imposed by Law 14,300/2022, considered the Legal Framework for Distributed Generation (DG) in Brazil [20], contribute to this. This law sanctioned alterations to the net metering mechanism, gradually phasing out compensation for specific tariff components until 2029. Then, local self-consumption becomes economically more favorable than relying on the energy compensation mechanism.

Considering these aspects, this paper proposes decision-making for a microgrid sizing composed of DERs, whose main load is based on FCSs located on highways. The methodology is based on long-term EV market projections and hourly load and generation time series, applied in a microgrid model. Firstly, the best sizing scenario for each year of the simulation horizon is obtained in the Homer Pro 3.14 software. Then, crossing all microgrid best annual scenarios and annual load and generation conditions in the time horizon results in five NZEB-based indexes. The last methodology block defines a mul-

ticriteria decision-making function to estimate the best global microgrid scenario for the time horizon.

1.1. Literature Review

Given the importance of FCSs for the widespread adoption of EVs, a series of studies have been conducted to optimize their allocation and sizing. Some authors prioritize meeting demand and queue formation. In contrast, others aim to reduce implementation and operation costs or focus on minimizing impacts on the distribution network in which they will be integrated.

In [21], a vast review was made on the optimization of microgrid sizing. Most of the works evaluate the impacts of their insertion in the distribution system using the most varied mathematical models. Works were found that share operational impacts, energy quality, financial issues, and environmental issues. In general, the works demonstrate that the creation of a microgrid aims to reduce the impact on the main grid where it is inserted since the aim is to generate energy in balance with consumption, aided by energy storage. Additionally, it is highlighted that critical loads require greater planning and operational complexity, which is the case of EV charging.

In [22], it was emphasized that the high energy requirements of an FCS and the challenges to consume forecasting impact the operations of the network connected. Through simulations conducted in a test system, they demonstrated that for a high penetration of EVs on highways, operational costs can rise due to interactions with the grid, leading to potential transmission overload. The authors suggest energy storage systems to avoid demand peaks as a mitigation method. The results found in [23] indicate that the grid reliability may be compromised by the increase in demand for EV charging if FCS planning is not done properly. The simulations performed demonstrated that the increase in floating EV charging intensifies power quality problems. In [24], a PV system was combined with the FCS to minimize the impacts caused by demand on the grid power quality. The result was positive, and the authors concluded that combining another alternative energy source in addition to PV can further improve the results.

In the simulations conducted by [25], PV generation reduced operating costs associated with EV charging and improved the technical characteristics of the grid near the charging station location. In [26], the authors used Neuro-Fuzzy and Particle Swarm Optimization to model an FCS, considering distributed energy resource integration. They employed load control and demand response to reduce the impacts on the local power grid. Charging management techniques were also employed to avoid negative consequences and optimize the utilization of the FCS in [27]. In these cases, highway charging has a particular challenge, and the charging decision is related to the vehicle's autonomy and the distance to the following FCS.

To provide better conditions for energy losses and minimize voltage level impacts on the grid, a metaheuristic approach to FCS sizing was used by [28], considering finding the best location for their installation. The study evaluates the presence of photovoltaic generation at various nodes of the studied system, which are not necessarily adjacent to the FCS and do not consider energy storage. In [29], was also applied the strategy of seeking the best location for the FCS to provide the best user conditions, traffic conditions, and grid loading. In these cases, it was applied a multi-objective function for the charging route and the power system impact optimization.

The study developed in [30] aimed to size the FCS by finding the best configurations of renewable energy and energy storage. However, cost-effectiveness was considered a constraint rather than an impact on the grid. Reference [31] considered grid impacts to search for a better microgrid configuration for FCSs localized in urban areas, but energy storage still needs to be considered. In [32], the best FCS configuration was sought, but only the best conditions for energy losses were considered regarding technical impact requirements. In [33], aimed to establish a coordinated system to reduce FCS load peaks using a PV system.

As can be noticed, many research studies are focused on optimizing the size of FCSs, and the impacts caused by high demand are also a concern. However, there is a need to simultaneously analyze various renewable energy sources and storage in a microgrid concept, effectively finding configurations to reduce the impact of FCS in the local grid, which can be achieved by applying NZEB concepts. Given the possibility of finding configurations that allow for reduced energy exchange with the grid and consequently reduce impacts, the application of NZEB indicators is considered highly relevant for studies involving the planning of FCS microgrids.

1.2. Paper Contributions

Based on these aspects, the paper's contributions are as follows:

- An FCS microgrid sizing planning analysis considering long-term and short-term effects related to EV market share growth and user behavior patterns since the load pattern is highly stochastic, mainly for low EV market share.
- A decision-making methodology considering the estimation of five quantitative indices based on NZEB concepts (Self-consumption (SC), Self-sufficiency (SS), Peak Export (PE), Peak Import (PI), and Grid Interaction Index (GII)) was applied to each best annual solution on different years in the simulation horizon, aiming to achieve network self-sufficiency. Also, a function relating these indexes makes it possible to define a ranking of better solutions from this technical point of view.
- A discussion about the microgrid modeled effects on power resulting curves in the grid connection point, aiming to estimate the Battery Energy Storage Systems (BESS) gains compared with scenarios just with distributed generation since the stochastic condition of generation and load. Quantile curves were used for this analysis, making it possible to estimate reverse flow scenarios.

1.3. Structure of the Paper

This paper is organized as follows: Section 2 presents the concept and indicators related to NZEB; Section 3 outlines the methodology used for optimizing and analyzing the FCS microgrid; Section 4 covers the data and results of the case study based on a real network in southern Brazil; and Section 5 presents the main conclusions drawn from this work.

2. Net Zero Energy Buildings

The concept of NZEB has become very popular and is directly associated with the intelligent and sustainable development of electrical networks [17]. In this sense, it is also a strategy for microgrid sizing planning. In summary, the term means that in a given building (or location), the total energy used annually equals the total sum of renewable energy produced [34]. Aiming to optimize the use of local DERs, NZEB can contribute to the context of energy planning for microgrids connected to a primary grid, as it advocates for their independence, limiting possible negative impacts on the Energy Quality of the distributor [35]. In this way, reference [36] emphasizes that the NZEB concept defines a primary criterion for the definition of the microgrid and subsequent analyses, whereby:

- The amount of generated energy should be as close as possible to the amount consumed locally, considering an annual period. Mathematically, this criterion can be defined by Equation (1).

$$\sum_{i=1}^n E_G \cong \sum_{i=1}^n E_C \quad (1)$$

where, E_G is the amount of generated energy, E_C is the amount of consumed energy, and n is the number of hours in the period.

The NZEB concept is applied to energy planning in buildings or microgrids. In [19,37,38], it was considered NZEB to evaluate the performance of residential buildings, considering PV or the inclusion of energy storage systems and other sources. The criteria of NZEB, along

with technical-economic aspects, were applied by [39] to determine the self-sufficiency of microgrids, but without considering the participation of EVs.

Another justification for applying NZEB is that countries like Germany, China, Japan, and Italy have been introducing policies with greater incentives for prosumers with self-consumption than net metering, as supported by the NZEB concept [16]. A similar path has been followed in Brazil, starting from Law 14.300/2022 [20].

More recently, the concept has become even more popular because, since 2021, all new buildings constructed in Europe must comply with NZEB concepts [40], prioritizing the use of renewable energies.

In this context, considering the configuration of microgrids, one can observe the applicability of the NZEB concept for the energy planning of FCSs' operation on highways, aiming to optimize the use of local DERs and limit the impacts on the primary distribution grid, which is the overall objective of this work. However, it is necessary to characterize the NZEB indicators that assess the operation of a specific microgrid, in this case, the FCSs. It is worth noting that these indicators are divided into two categories: Load Matching and Grid Interaction.

2.1. Load Matching Indexes

According to [36], the indexes in this category allow for assessing the degree of utilization of locally generated energy in comparison to energy demand. Furthermore, they can be divided into two subcategories: self-consumption (SC) and self-sufficiency (SS). Figure 1 shows a superposition of load (the sum of areas A and C), generation (represented by the grouping of areas B and C), and the self-consumed energy zone (represented only by area C), used to explain the next subsections.

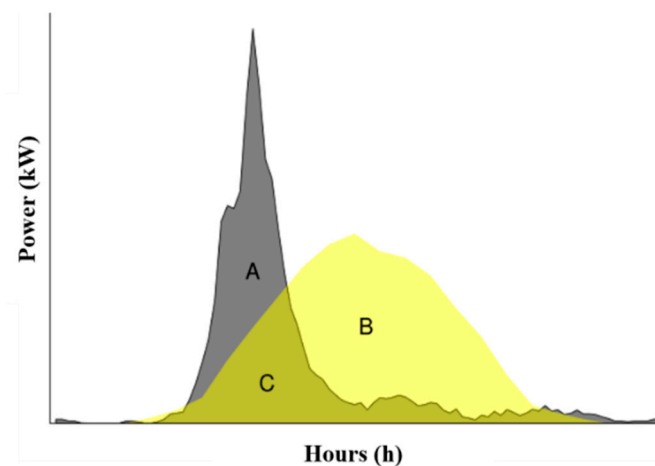


Figure 1. Load profiles (A + C), generation (B + C), and self-consumed portion (C) of the generated energy for defining Load Matching indicators.

2.1.1. Self-Consumption (SC)

The SC index represents the portion of locally generated energy that is being self-consumed by the local load. Thus, observing Figure 1, the SC indicator is defined by Equation (2).

$$SC = \frac{C}{B + C} \quad (2)$$

where (B + C) refers to the generation profile and C refers to self-consumed portion of generation profile, as shown in Figure 1. Furthermore, considering the formal mathematical definition of the SC indicator, the instantaneous load is defined as $L(t)$, the instantaneous local generation as $P(t)$, and the storage as $S(t)$, with $S(t) < 0$ when charging and $S(t) > 0$ discharging. Thus, $M(t)$ represents the amount of generation power being self-consumed

by the load, always being the minimum between $L(t)$ and $P(t) + S(t)$, as defined in Equation (3).

$$M(t) = \{L(t), P(t) + S(t)\} \quad (3)$$

Therefore, the SC index is defined by Equation (4). The typical integration period (between t_1 and t_2 , the start and end time of the simulation, respectively) is one year, which, according to [16], is sufficient to consider seasonal variations and minimize short-term random fluctuations in load and generation. Additionally, it is desirable for φ_{SC} to be as close to one, as the maximum function result.

$$\varphi_{SC} = \frac{\int_{t=t_1}^{t=t_2} M(t)dt}{\int_{t=t_1}^{t=t_2} P(t)dt} \quad (4)$$

2.1.2. Self-Sufficiency (SS)

The SS index determines how adequately the locally generated energy meets the load's energy needs. Therefore, analyzing Figure 1, Equation (5) can simplify the SS indicator.

$$SS = \frac{C}{A + C} \quad (5)$$

Additionally, Equation (6) mathematically defines the SS indicator by φ_{SS} . Like the SC index, the integration period is one year for the same reasons set out above and also should be near one to maximize the function.

$$\varphi_{SS} = \frac{\int_{t=t_1}^{t=t_2} M(t)dt}{\int_{t=t_1}^{t=t_2} L(t)dt} \quad (6)$$

2.2. Grid Interaction Indexes

The indexes presented in the next subsections handle aspects of energy interaction between the microgrid and the primary grid, evaluating negative impacts as well. Thus, the main indexes used to assess the impact on the primary grid are Peak Export (PE), Peak Import (PI), and Grid Interaction Index (GII) [19]. For this category, the values should be as low as possible.

2.2.1. Peak Export (PE)

PE is one of the indexes that quantify the grid impact. The estimation is found according to a defined limit for the power exported from the microgrid to the main grid. In general, this limit is based on contractual relations with the local utility or distribution system operator, e.g., demand contracts. Through an iterative process for the total number of simulation hours, every time step that the power exported (P_{exp_n}) is greater than the power limit ($P_{exp_{lim}}$), the counter variable t_{exp} is increased, according to Equation (7).

$$\text{if } P_{exp_n} > P_{exp_{lim}}, \quad t_{exp} = t_{exp} + 1 \quad (7)$$

The PE index is calculated by the ratio of t_{exp} and the total simulation points of the analysis period, in this case, 8760 h (one-year analysis), according to Equation (8).

$$PE = \frac{t_{exp}}{8760} \quad (8)$$

2.2.2. Peak Import (PI)

Similar to the PE definition, PI is the index measuring the time when the imported power exceeds its limit during a year. The imported power limit ($P_{imp_{lim}}$), is also defined

according to contractual matters. The time in hours (t_{imp}) in which the imported power (P_{imp_n}) is greater than the limit power is counted according to Equation (9).

$$if P_{imp_n} > P_{imp_{lim}}, t_{imp} = t_{imp} + 1 \tag{9}$$

The PI index is calculated by the ratio of this time (t_{imp}) in relation to the total time steps of the simulation horizon, according to Equation (10).

$$PI = \frac{t_{imp}}{8760} \tag{10}$$

2.2.3. Grid Interaction Index (GII)

The GII indicates the variability of the energy exchange between the microgrid and the main grid through the standard deviation (sd) of the net energy of each hour i in relation to the global maximum of the study horizon. Then, it is possible to perceive the dispersion around the average of the power exchange between the FCS and the main grid. The GII is defined from Equation (11).

$$GII = sd \left(\frac{|P_{imp_i} - P_{exp_i}|}{|P_{imp} - P_{exp}|} \right) \tag{11}$$

It is essential to emphasize that this indicator is a measure of dispersion. Thus, low values indicate a more constant energy exchange, while higher values indicate fluctuations in this exchange [41].

3. Microgrid Self-Consumption and Self-Sufficiency Optimization

This section presents the methodology developed for microgrid sizing planning, whose main loads are FCSs located on highways. The main objective is to optimize the microgrid’s self-consumption and self-sufficiency over time while limiting the distribution network’s impacts. The Load Matching and Grid Interaction Indexes are applied, allowing the assessment of the degree of independence and the microgrid energy operation impacts on the power distribution grid. The block diagram of the methodology is presented in Figure 2.

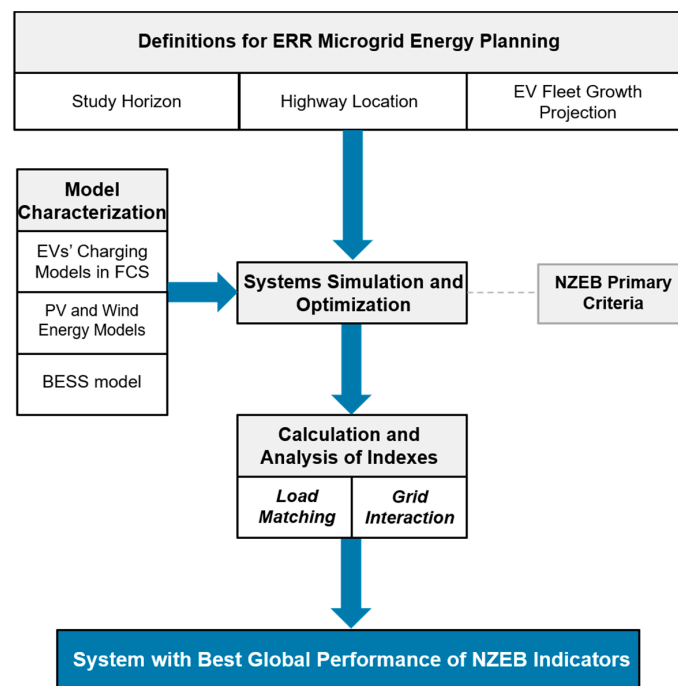


Figure 2. Block diagram of the methodology.

The proposed methodology is divided into five main blocks. In the first block, definitions regarding the FCS planning are made, delimiting the study to be carried out. With the load and generation profiles defined from the models, simulation and optimization are performed using the software Homer Pro 3.14, allowing the classification of microgrid systems scenarios that satisfy the primary NZEB criterion. Then, for each of these classified systems, the indicators are calculated and analyzed through histograms. Finally, it is defined as the best microgrid system scenario according to the general indicators performance. For the best performance in terms of energy balance conditions, Homer Pro 3.14 is used to size a BESS system to reduce main grid impacts more. The structure for FCS's microgrid in this study considers a topology connected to a distribution grid, along with DERs such as PVs, wind turbines, and BESS, as illustrated in Figure 3.

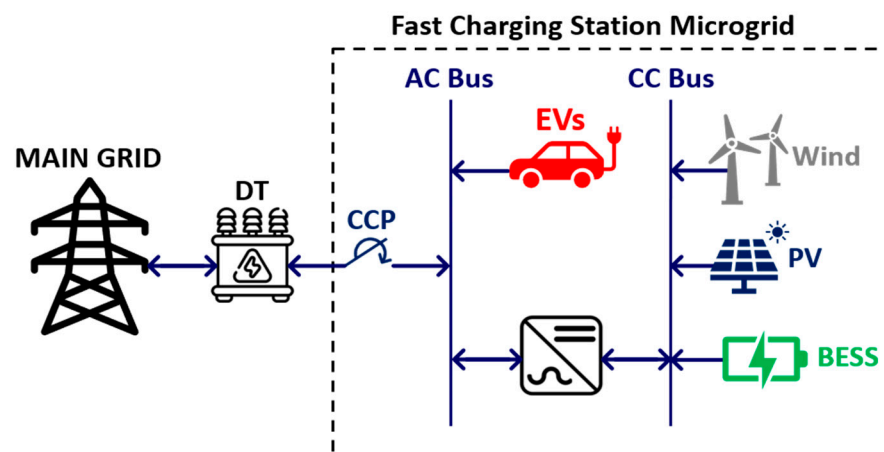


Figure 3. FCS's Microgrid structure.

In this microgrid structure, the main grid and the FCS are connected to the AC bus, while the wind turbines, photovoltaic modules, and batteries are connected to the DC bus. Additionally, a bidirectional inverter enables energy transfer between the AC and DC buses. Regarding EV chargers, it was assumed that they are connected directly to the AC bus since the current equipment technology applies inverter-based DC chargers. Moreover, considering different DC charging voltage levels, a DC-DC converter is mandatory for DC chargers connected to DC buses. As a boundary condition, the case study will not consider inverter efficiencies, which are generally more significant than 95%. However, in a practical case, increasing the number of power electronics devices decreases microgrid efficiency.

To perform the energy planning of the microgrid in the study horizon, the placing and the load demand growth are associated with the growth of the EV fleet. Furthermore, the final results are influenced by the shape model of loads, generation systems, and energy storage, as indicated in Figure 2.

The focus of this study is based on the energy planning of the microgrid, seeking to optimize its energy balance. It justifies the choice of hourly load curve models (hourly average power), allowing variability in the load and generation sources, as well as seasonality aspects. The use of curves with a shorter time scale is important and must be applied for models focusing on real-time operation (e.g., energy management systems), which is not the focus of this study.

3.1. Microgrid Elements Modeling

3.1.1. Load Profiles

According to the problem dynamics, the load models are expressed on an hourly basis, allowing load variations throughout the evaluated days. The hourly demands of EVs in FCSs are described using the curves from the model proposed by [10]. The model combines user patterns and probability concepts. The block diagram of the model is presented in Figure 4.

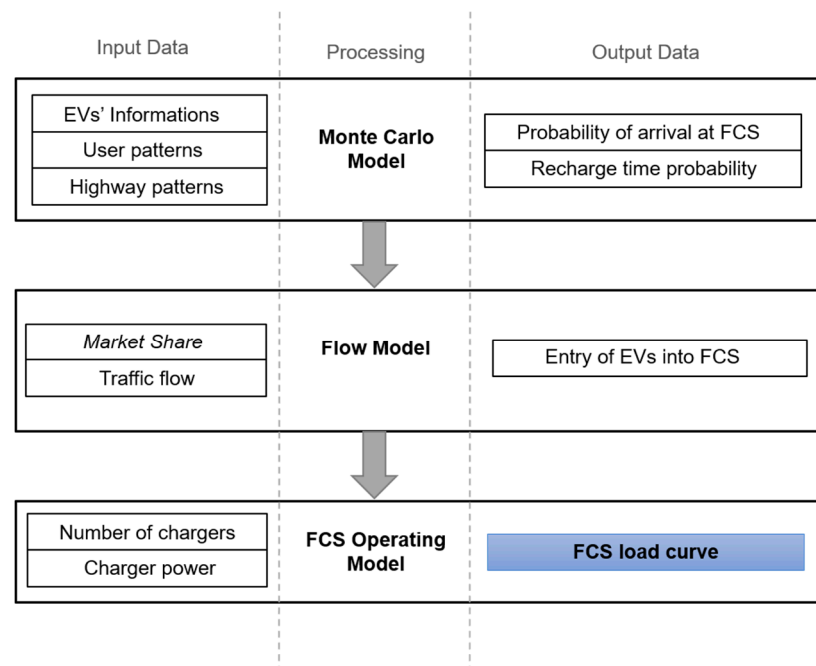


Figure 4. Block diagram of FCSs' load curves modeling.

This model considers the stochastic nature of variables surrounding the recharging of EVs at FCSs, such as aspects related to the EVs, like user behavior, highway patterns, and market shares, as well as station aspects, like the number and power of EV fast chargers. The data for each stage must be adjusted according to the characteristics of the studied region, for example, the most common types of EVs in the area, traffic flow on highways, and market share indexes. Further details regarding the mathematical modeling for FCS load curves can be found in [10].

3.1.2. PV Generation Profile Modeling

In this study, it is applied a parametric model for PV generation, mainly proportional to the global solar radiation and also the environmental temperature effect [42]. The system's output power P_{PV} is expressed according to Equation (12).

$$P_{PV} = Y_{PV} \times f_{PV} \times \left(\frac{G_T}{G_{T,STC}} \right) \times [1 + \alpha_P (T_C - T_{C,STC})] \quad (12)$$

In this equation, Y_{PV} is the nominal power of the PV system, in kW; f_{PV} is the loss factor; G_T is the incident solar radiation on kW/m²; $G_{T,STC}$ is the solar radiation under Standard Test Conditions (STC), corresponding to 1 kW/m²; α_P is the power temperature coefficient in %/°C; T_C represents the environment temperature in °C and $T_{C,STC}$ denotes the environment temperature under STC, corresponding to 25 °C.

This study uses data from the National Aeronautics and Space Administration (NASA) database to obtain primary radiation and temperature data for simulating the PV model [43].

3.1.3. Wind Generation Profile Modeling

The wind generation model is considered a parametric model for the wind turbine. The output power P_{EOL} is calculated through three steps: (i) calculating the wind speed at the turbine height based on Equation (13); (ii) determining the turbine output power under Standard Patterns of Temperature and Pressure (STP) conditions, based on the turbine power curve; and (iii) calculating the output power for the local air density using Equation (14).

$$U_{hub} = U_{anem} \cdot \frac{\ln(Z_{hub}/Z_0)}{\ln(Z_{anem}/Z_0)} \quad (13)$$

where, U_{hub} is the wind speed at the hub height of the wind turbine, in m/s; U_{anem} is the wind speed, at the anemometer height, in m/s; Z_{hub} is the hub height of the wind turbine, in m; Z_{anem} is the height of the anemometer, in m; and Z_0 is the surface roughness length, in m.

$$P_{EOL} = \left(\frac{\rho}{\rho_0} \right) \cdot P_{EOL,STP} \quad (14)$$

where, P_{EOL} is the output power of the wind turbine, in kW; $P_{EOL,STP}$ is the wind turbine power at STP, in kW; ρ is actual air density, in kg/m³; and ρ_0 is the air density at standard temperature, corresponding to 1.225 kg/m³.

Like the PV model, the wind generation model considers the NASA database to obtain primary wind resource values [43].

3.1.4. Energy Storage System Modeling

According to the control flexibility, this paper considers a Battery Energy Storage System (BESS) as the storage model. It is responsible for storing and dispatching energy with a specific efficiency while respecting limits related to charging and discharging, such as Depth of Discharge (DoD) or State of Charge (SoC), and the amount of energy that can circulate through the storage system before replacement. In this work, the lithium battery replicates a storage model with a flat capacity curve, requiring only the nominal capacity in Ampere-hour (Ah) to be inputted into the simulation software.

Another essential characteristic of the BESS is the dispatch strategy, which sets its operation guidelines. This study adopts the load-following strategy, allowing the BESS to be charged only from local renewable sources (PV and wind energy), aligning with the established objectives.

The BESS operation can be expressed by Equation (15).

$$L_{FCS} = P_{FCS} - P_{PV} - P_{EOL} \quad (15)$$

where, L_{FCS} is the power net curve of the FCS, the P_{FCS} is the demand, the P_{PV} is the local photovoltaic generation, and the P_{EOL} is the local wind generation. When local power generation is greater than demand (P_{FCS}), the L_{FCS} is less than zero. If the local generation is smaller than charger demand, the L_{FCS} is positive. Also, the BESS operation still depends on the restrictions represented in Equations (16)–(18).

According to Equation (16), when the net power is negative and the BESS SoC is less than the maximum (1), the BESS is charged. By the Equation (17), if L_{FCS} is less than zero and the BESS SoC is maximum, a BESS charging event is not allowed and the remaining energy is injected in the grid. Finally, like Equation (18), when the local generation is smaller than the demand and the BESS SoC is greater than 20%, the load is partially or totally supplied by the BESS.

$$L_{FCS} < 0 \text{ and } SoC_{BESS} < 1, \quad BESS_{FCS}(t) \leq L_{FCS}(t) \quad (16)$$

$$L_{FCS} < 0 \text{ and } SoC_{BESS} = 1, \quad BESS_{FCS}(t) = 0 \quad (17)$$

$$L_{FCS}(t) > 0 \text{ and } SoC_{BESS} > 0.2, \quad BESS_{FCS}(t) > 0 \quad (18)$$

In this context, this model allows for storing energy when generation from PV and wind energy exceeds the load, dispatching the stored amount when the opposite occurs, respecting the limits of 20% to 100% defined for the SoC. Therefore, the considered BESS model increases the level of energy reliability and is a good strategy for peak shaving at the common connection point of the microgrid.

3.2. Microgrid System Optimization

Simulation software can be employed to determine microgrid configurations. It allows the system's behavior to be determined through various iterations [39]. The HOMER Pro software stands out for its applicability in microgrid simulations [44].

Through the modeling of DERs, Homer Pro simulates microgrid operation by calculating the energy balance to determine the power flow between load, generation, and BESS [35]. Reference [45] also emphasizes that Homer Pro includes necessary steps for structuring a microgrid, from simulation to optimization. In the simulation stage, the software simulates the system's behavior for each hour of an annual period, demonstrating possible configurations to meet the load. In the optimization stage, the software seeks configurations that consider constraints that are user-defined, such as the size of DER and demand satisfaction, aiming for the best technical-economic results.

The load curve must be initially defined for proper modeling, allowing the software to explore the "k" possible generation configurations to meet it. These configurations are displayed in a list, where it is possible to visually inspect each simulation step for the annual period or export the simulated data.

This study considers a NZEB concept. The primary condition for determining the system must be that local generation approximates the annual consumption of the FCS load. Thus, the system that satisfies the primary NZEB criteria is analyzed within the possible software configurations.

As the proposed model considers the load growth on the FCSs, a different system must be defined for each year "i" of the market share projection. This ensures the systems are tailored to meet the changing load conditions over time. Therefore, considering a 10-year horizon of a given growth projection, 10 generation systems must be defined, each meeting the respective load condition.

This simulation and optimization stage of the systems can be represented through the flowchart shown in Figure 5.

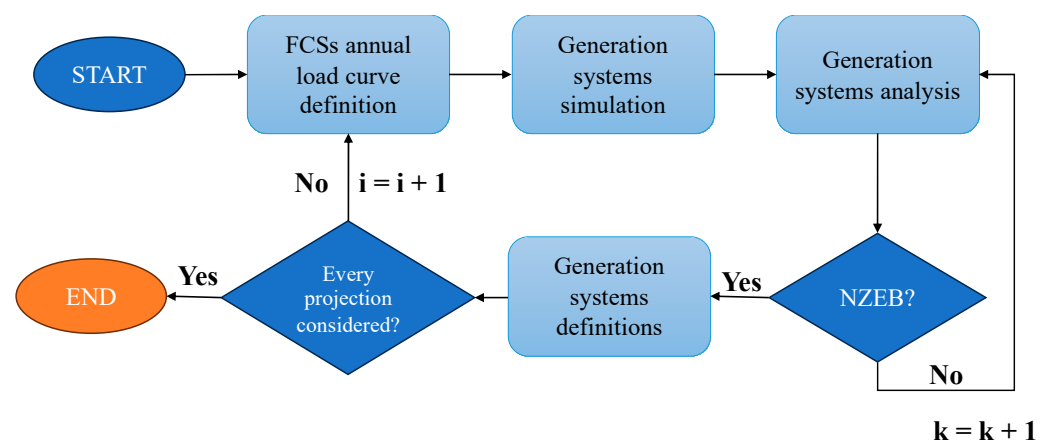


Figure 5. Flowchart for microgrid systems simulation and optimization.

3.3. Indexes Calculation and Analysis

Firstly, Homer Pro software is used to generate analysis scenarios. These are defined based on the primary NZEB criterion. From there, the other NZEB indexes can be calculated and analyzed. An annual step was used for the simulations to allow fittings on generation and load variations throughout the year due to seasonality and other stochastic factors. This study considers five NZEB indexes for the microgrid's planning and analysis, two from the Load Matching group (SC and SS) and three from the Grid Interaction category (PE, PI, and GII). It is worth noting that both categories are required to assess the microgrid's degree of self-sufficiency and the impacts of its integration into the primary grid.

As already defined, within the framework of NZEB, accounting for the increase in EV load along the highway implies defining different systems to meet each market share.

Therefore, the analysis of indexes should consider each system over the entire study horizon to assess the overall performance of the indicators. Thus, if the study horizon is 10 years, the primary NZEB criterion defines 10 systems evaluated across the entire load growth projection.

The results are presented using frequency histograms to classify NZEB indexes into value ranges defined in Table 1.

Table 1. Rating bands (R) for analyzing the NZEB index.

Index	R1	R2	R3	R4	R5
Self-consumption (SC)					
Self-sufficiency (SS)					
Peak Export (PE)	0–0.20	0.21–0.40	0.41–0.60	0.61–0.80	0.81–1.00
Peak Import (PI)					
Grid Interaction Index (GII)					

It is worth noting that defining the values into 5 ranges is justified as it allows grouping the NZEB index results. Therefore, for each NZEB index, the system is evaluated considering the entire load projection and classified based on the frequency of occurrences. Thus, within the study horizon, it is possible to determine the number of years each microgrid configuration remained within the defined value ranges.

3.4. Selection of System with the Best Overall Index Performance

The final step of the methodology is selecting the system with the best overall performance of the NZEB indexes. With all calculations completed and after analyzing the index ranges, it determines the most beneficial microgrid sizing set. The analysis is performed using Equation (19), which adds the score of each system in each index evaluated and determines the best microgrid system. The sum of the index weights must always be 1. Moreover, based on decision-making, it is possible to determine different weights for each index according to importance levels. Changing the weights of each index, it is possible to evaluate the impact of this on the final result, carrying out a sensitivity analysis and improving the results, as will be shown in the case study. For each index, the score of different systems normalized by the maximum value is evaluated.

$$BEST\ SYSTEM = a * SC + b * SS + c * PE + d * PI + e * GIIs.t.a + b + c + d + e = 1 \quad (19)$$

The values of a , b , c , d , and e are the index weights. For each index, the score is also considered according to the frequencies and the impact of each of them. For example, for SC, it is considered that the higher the self-consumption, the better, so the systems with lower generation power will have a better score. Finally, the total score for each system is normalized by the total number of years in the planning horizon. Since the analysis is performed annually, the normalization is done by the number of steps in the planning horizon. This value can be changed according to the desired study horizon.

To apply the proposed methodology, a case study was conducted considering an FCS microgrid on a highway, considering a given projection of EV market shares in the southern region of Brazil over ten years.

4. Case Study

4.1. General Definitions and Scenarios

The proposed methodology was applied to a case study based on a segment of a real highway from Brazil, covering 241 km, illustrated in the diagram of Figure 6. This highway segment features 5 Connection Points (CP), representing entry and exit points of the highway, along with 3 FCS strategically located based on local infrastructure studies. Due to spatial and wind characteristics, FCS 2 is designated to be equipped with a microgrid connected to the primary grid [46].

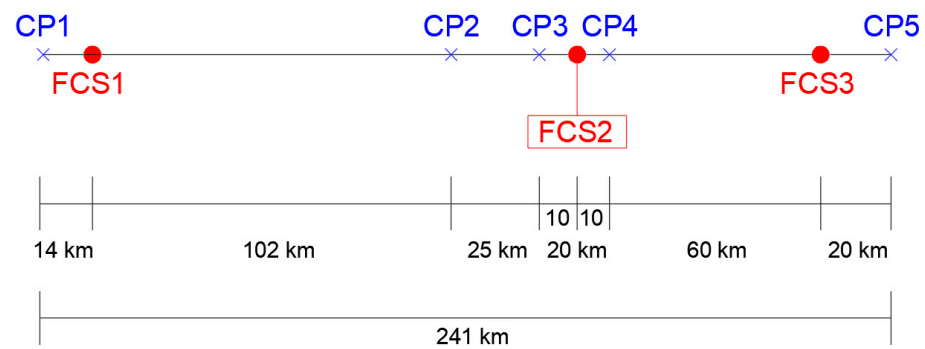


Figure 6. Diagram of the highway section applied to the case study.

A ten-year study horizon is proposed (2023 to 2032), based on the projected growth of EVs on Brazilian highways as elaborated by [2]. This simulation period is justified by the typical lifespan of a BESS and technological advancements over time. Regarding market shares, it was considered that EVs represent 0.1% of the total vehicles in circulation initially, increasing to 5% by the end of the study horizon.

For the load curves, the model from [10] was applied, using input data related to EVs in the studied region, such as EV models and their autonomy, as well as range anxiety rates of 2–5% for the minimum State of Charge (SoC) and 90–95% for the initial SoC. Traffic information from [47] was used for traffic data. This resulted in the average load profile for years 1, 5, and 10, reflecting the growth in demand at the FCS and following EV adoption trends. Alongside the load curves obtained for the decade, monthly averages of primary resources for PV and Wind generation data from [43] were applied to define the systems and analyze the indexes.

To compose the microgrid were considered three fast chargers, 550 Wp photovoltaic modules, 24 kW wind turbines, and 100 kWh BESS. The main parameters of the microgrid components are shown in Table 2.

Table 2. Main characteristics considered for the Microgrid components.

Photovoltaic Module	
Nominal power (kW)	0.55
Efficiency (%)	20
Operating Temperature (°C)	47
Temperature Coefficient	−0.35
System Loss Factor (%)	80
Wind turbine module	
Nominal power (kW)	24
Efficiency (%)	95
Nominal Speed (m/s)	9
Starting Speed (m/s)	2.3
Cutting Speed (m/s)	20
Storage Module	
Nominal Capacity (kWh)	100
Nominal Capacity (Ah)	187
Efficiency (%)	90
Maximum Charge Current (A)	167
Maximum Discharge Current (A)	500

4.2. System Settings and Analysis of Indexes

As already mentioned, the primary condition of NZEB is that the energy consumed by the load should be as close as possible to the power generated locally. Ten systems were obtained to meet the equivalent energy consumption for each year's market share. The results were analyzed for the entire study horizon for each system, totaling 100 scenarios. Initially, energy storage was not considered. In a second analysis, BESS was added to the best system defined for operational behavior comparisons. The systems obtained from the simulation with the primary NZEB criterion to meet the ten market shares are shown in Table 3. This way, the self-consumption and self-sufficiency indexes and their impacts on the initial grid were calculated and analyzed for each system.

Table 3. Results obtained from Homer Pro simulation.

System (Year)	Market Share (%)	System's Settings	Consumed Energy (kWh)	Generated Energy (kWh)
S1	0.10	9 PV modules PV, 4.95 kWp	6263	6367
S2	0.20	16 PV modules, 8.80 kWp	11,210	11,319
S3	0.50	39 PV modules, 21.45 kWp	27,426	27,590
S4	1.00	76 PV modules, 41.80 kWp	53,606	53,765
S5	1.50	113 PV modules, 62.15 kWp	79,645	79,940
S6	2.00	143 PV modules, 78.65 kWp	10,095	101,163
S7	2.50	174 PV modules, 95.70 kWp	123,005	123,094
S8	3.00	71 PV modules, 39.05 kWp+1 wind turbine, 24 kWp	147,147	147,645
S9	4.00	128 PV modules, 70.40 kWp+1 wind turbine, 24 kWp	187,575	187,969
S10	5.00	44 PV modules, 70.40 kWp+2 wind turbines, 24 kWp	225,884	225,961

4.2.1. Self-Consumption Analysis

The SC index calculates the expected self-consumption rate, and values closer to one are suitable. The results obtained for SC over the decade are presented in Table 4, showing the number of years from the simulation horizon in which the SC index result is equivalent to each rating band, based on Table 3 scenarios.

Table 4. Occurrence in years per frequency range for SC index for the simulated systems.

Rating Band	Range	Self-Consumption (SC)									
		S1	S2	S3	S4	S5	S6	S7	S8	S9	S10
		Frequency									
R1	0.0–0.2	2	2	2	2	3	3	3	3	3	4
R2	0.2–0.4	1	1	1	2	1	2	3	2	3	4
R3	0.4–0.6	0	1	1	1	3	3	2	3	3	2
R4	0.6–0.8	2	1	3	3	2	2	2	2	1	0
R5	0.8–1.0	5	5	3	2	1	0	0	0	0	0
Final Score		0.74	0.72	0.68	0.62	0.54	0.48	0.46	0.48	0.44	0.36

Considering that high SC indexes are better for the power grid, for each range the frequency values are multiplied by the maximum limit of the range and normalized by the maximum score (10). The score of each system is given by the sum of all occurrences. The system scores are highlighted by the color gradient. The higher the final score is, the warmer the color. The opposite is similar, the lower the final score is the colder the color.

As expected, systems with lower generation capacity remain longer in rating bands with higher values. This happens because of the evolution of both market shares and the load and the coincidence between the load and the generation curve, as shown in Figure 7. Given the annual hourly averages, it is observed that the load curve for year 10 remains higher than the generation values throughout the time for S1.

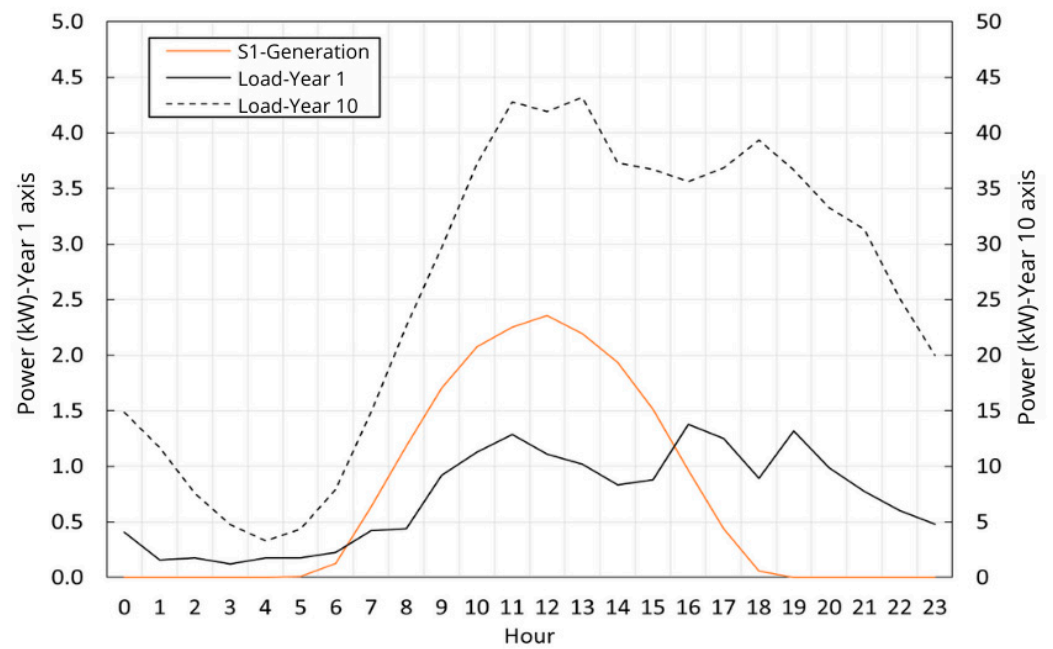


Figure 7. Average hourly load and generation profiles for FCS2.

As Table 4 shows, S1 remained in the higher ranges (R4 and R5) for the most extended period (7 years). S2 and S3 remained in these two ranges for six years, while the least successful system for SC was S10, which did not reach R4. It is worth noting that later, with the integration of BESS, this indicator should increase for all systems.

4.2.2. Self-Sufficiency Analysis

The SS index evaluates the efficiency of local generation in meeting the microgrid’s load. The frequency results are shown in Table 5.

Table 5. Occurrence in years per frequency range for SS index for the simulated systems (S).

Rating Band	Range	Self-Sufficiency (SS)									
		S1	S2	S3	S4	S5	S6	S7	S8	S9	S10
Frequency											
R1	0.0–0.2	10	10	5	0	0	0	0	0	0	0
R2	0.2–0.4	0	0	5	7	5	3	2	0	0	0
R3	0.4–0.6	0	0	0	3	5	7	8	4	2	2
R4	0.6–0.8	0	0	0	0	0	0	0	6	6	6
R5	0.8–1.0	0	0	0	0	0	0	0	0	2	2
Final Score		0.2	0.2	0.3	0.46	0.5	0.54	0.56	0.72	0.8	0.8

Higher values were demonstrated in systems with more significant generation potential for the SS index. As it is possible to notice, the system with the lowest generation capacity, S1, remained in category R1 throughout the study horizon. In contrast, the most extensive system, S10, stayed between categories R3 and R5 throughout the period.

4.2.3. Peak Export Analysis

The objective of Grid Interaction indexes is to measure the microgrid’s impact on the primary grid. Values closer to zero are preferable to minimize this impact. The Peak Export (PE) index determines the power exported by the microgrid beyond a set limit. In this study, a limit of 10 kW was adopted based on the assumptions of [19]. The results for PE over the decade are shown in Table 6.

Table 6. Occurrence in years per frequency range for PE index for the simulated systems.

Rating Band	Range	Peak Export (PE)									
		S1	S2	S3	S4	S5	S6	S7	S8	S9	S10
		Frequency									
R1	0.0–0.2	10	10	10	8	6	4	2	0	0	0
R2	0.2–0.4	0	0	0	2	4	6	8	4	2	1
R3	0.4–0.6	0	0	0	0	0	0	0	4	4	5
R4	0.6–0.8	0	0	0	0	0	0	0	2	4	4
R5	0.8–1.0	0	0	0	0	0	0	0	0	0	0
Final Score		1	1	1	0.96	0.92	0.88	0.84	0.64	0.56	0.54

In the case of the PE index, smaller systems are the most successful. So, the frequency of occurrence in band 1 was multiplied by 1 and in band 5 by 0.2, unlike the previous indices.

In the case of the PE index, systems with greater generation capacity export energy for longer, such as S1, which remains in the F1 range throughout the study horizon. To find systems that cause less impact on the grid, those with lower power would be more successful. However, considering that the objective is to find the largest possible system that causes the least impact on the network, S6 and S7, for example, present satisfactory results, as they do not reach R3 during the analyzed period.

4.2.4. Peak Import Analysis

As mentioned, the PI measures exceed the power import limit from the primary grid. Following the previous analyses, 10 kW was adopted as the limit. The calculated frequency and value range results are shown in Table 7.

Table 7. Occurrence in years per frequency range for PI index for the simulated systems.

Rating Band	Range	Peak Import (PI)									
		S1	S2	S3	S4	S5	S6	S7	S8	S9	S10
		Frequency									
R1	0.0–0.2	3	3	4	4	4	5	5	6	7	7
R2	0.2–0.4	3	3	2	3	4	3	3	3	3	3
R3	0.4–0.6	3	3	3	3	2	2	2	1	0	0
R4	0.6–0.8	1	1	1	0	0	0	0	0	0	0
R5	0.8–1.0	0	0	0	0	0	0	0	0	0	0
Final Score		0.76	0.76	0.78	0.82	0.84	0.86	0.86	0.9	0.94	0.94

The analysis of the PI index shows that smaller systems present a higher dependency on energy importation. As observed, S1, S2, and S3 reach R4, indicating that the imported power exceeded 10 kW in one year from 60% to 80% of the period. Meanwhile, S10 is at most 40% (R2) throughout the decade and has the highest score. Additionally, it should be noted that adding ESS may further improve results for the PI index, as it should allow better use of the energy generated outside of the period of greatest consumption.

4.2.5. Grid Interaction Analysis

The GII index demonstrates the variability of energy exchange between the microgrid and the primary grid, relating to probability distributions and net energy concerning the global maximum of the period. Therefore, the GII index measures how dispersed around the mean the power exchanged between the FCS and the distribution grid can be, with low values being desirable. The results for the GII of the systems are shown in Table 8.

Table 8. Occurrence in years per frequency range for GII index for the simulated systems.

Rating Band	Range	Grid Interaction Index (GII)									
		S1	S2	S3	S4	S5	S6	S7	S8	S9	S10
		Frequency									
R1	0.0–0.2	10	10	10	9	8	7	6	10	10	6
R2	0.2–0.4	0	0	0	1	2	3	4	0	0	4
R3	0.4–0.6	0	0	0	0	0	0	0	0	0	0
R4	0.6–0.8	0	0	0	0	0	0	0	0	0	0
R5	0.8–1.0	0	0	0	0	0	0	0	0	0	0
Final Score		0.2	0.2	0.2	0.26	0.32	0.38	0.44	0.2	0.2	0.44

Analyzing the GII calculated for the systems, it is observed that systems S1, S2, S3, S8, and S9 exhibit the lowest dispersions over the study horizon, with all configurations remaining equal to or below 20% (R1) throughout the period. This can be explained by the fact that these systems may be either undersized or oversized for most of the study period, resulting in a higher average power imported or exported with minimal variations. On the other hand, systems S4, S5, S6, S7, and S10, mostly remaining below 20% (R1), also reached the range between 21 and 40% (R2) in some years. For these cases, where there are lower averages of power import and export, there are variations due to peak loads and generation, causing some data points to deviate from the average.

In summary, when analyzing the performance of the Systems, it can be observed that for each index analyzed, there is a winner. Therefore, to analyze the best system, it is necessary to weigh all the results and find a more satisfactory system according to the primary grid configuration.

4.2.6. Determination of the Best System and Sensitivity Analysis

The best system is determined according to the index relevance for each primary grid, defined in Equation (19), just changing the multipliers of each index. It makes it possible to have a broader view, providing a more appropriate system choice.

For sensitivity analysis purposes, five scenarios were created, in which the multipliers a , b , c , d and e from Equation (19) are changed, assuming some needs of the main grid of the case study. In this way, it is possible to perform a sensitivity analysis of the results. Table 9 presents the multipliers for each scenario.

Table 9. Sensitivity analysis scenarios.

Scenario	SC	SS	PE	PI	GII
	a	b	c	d	e
Scn 1	0.2	0.2	0.2	0.2	0.2
Scn 2	0.2	0.2	0.1	0.3	0.2
Scn 3	0.2	0.2	0.3	0.1	0.2
Scn 4	0.1	0.25	0.25	0.2	0.2
Scn 5	0.1	0.1	0.2	0.2	0.4

Following Table 9, scenario 1 (Scn 1) is the general condition when the same weight is considered for all indices (0.2). The scenario 2 (Scn2) considered that for the main grid where the microgrid will be connected, it is more important to avoid energy imports than exports; therefore, greater weight was considered for the PI, while the PE was reduced. In scenario 3 (Scn 3), the opposite was considered: greater weight for PE and lesser weight for PI. For scenario 4 (Scn 4) an intermediate condition was adopted, in which the importance of SS and PE is considered and the concern with SC is reduced. In the fifth scenario (Scn 5), the GII index is the main index, with a weight of 0.4, limiting exchanges with the network.

The results of the five scenarios for each system are shown in Table 10.

Table 10. Results of applying Equation (19) for the five scenarios in Table 9.

System	Scenario				
	Scn 1	Scn 2	Scn 3	Scn 4	Scn 5
S1	0.580	0.556	0.604	0.566	0.526
S2	0.576	0.552	0.600	0.564	0.524
S3	0.592	0.570	0.614	0.589	0.534
S4	0.616	0.602	0.63	0.625	0.552
S5	0.608	0.600	0.616	0.625	0.552
S6	0.604	0.602	0.606	0.627	0.554
S7	0.600	0.602	0.598	0.624	0.554
S8	0.588	0.614	0.562	0.608	0.508
S9	0.588	0.626	0.550	0.612	0.504
S10	0.584	0.624	0.544	0.615	0.524

As can be seen in Table 10, in Scn 1, the most relevant system is the S4, and it is very close to systems S5, S6, and S7. For Scn 2, systems with greater power generation capacity are more successful, since more importance was considered for the PI than for the PE, which explains why the S9 has a higher score. In Scn 3, the lowest export to the primary grid was considered so that the smallest systems stand out, and then S4 was better classified. The results of Scn 4, in which greater importance was considered to preserve the SS and PE, S6 stands out, being very close to systems S4, S5, and S7. In Scn 5, where more weight is given to the limitations of exchanges, imports, and exports, systems S6 and S7 are tied, followed by systems S4 and S5.

Another infinite number of possibilities can be tested according to the priorities of the primary grid where the system will be inserted. This variability in the analysis allows for the evaluation of numerous conditions, bringing robustness to the model.

Still from Table 10, for the scenarios analyzed, it can be observed that the highest scores were concentrated in intermediate power scenarios. Thus, S6 was considered to evaluate the influence of the insertion of the energy storage system in the reduction of prosumer impacts, since it has the highest power among the better results evaluated.

4.3. Integration of BESS in the Microgrid

For comparative analysis and impact assessment, a lithium-based BESS with a capacity of 100 kWh was simulated for S6. The Homer Pro software facilitated the determination of power specifications, identifying the most advantageous solution regarding import and export dynamics while factoring in cost-effectiveness considerations. The operational strategy employed is load-following, with a state of charge range between 20% and 100%, looking to ensure the system's longevity and efficiency.

After integrating the BESS, the respective indexes were simulated and compared with the previous results (without the BESS) for S6.

4.3.1. Impact Assessment on the Indexes

All the indexes were recalculated considering the inclusion of the BESS. In Table 11, a comparison of the frequency data for the indexes is provided for S6 with and without the BESS. The results were analyzed individually.

In summary, based on Table 11, the implementation of the BESS improves all indexes. Regarding SC, without the BESS, the R5 (range between 0.81 and 1.00) was not reached. Including the storage system, the simulation indicated four years within this range while maintaining two years within R4 (range between 0.61 and 0.80). Additionally, the time spent in the range R1 (0.00 to 0.20) is reduced. Overall, including the BESS allows for a minimum of 61% self-consumption of the generated energy for at least six years.

Table 11. Occurrence in years per frequency range for indicators in S6 without and with BESS.

Rating Band	Range	System 6									
		SC		SS		PE		PI		GII	
		-	BESS	-	BESS	-	BESS	-	BESS	-	BESS
Frequency											
R1	0.0–0.2	3	2	0	0	4	7	5	7	7	7
R2	0.2–0.4	2	1	3	0	6	3	3	2	3	3
R3	0.4–0.6	3	1	7	3	0	0	2	1	0	0
R4	0.6–0.8	2	2	0	3	0	0	0	0	0	0
R5	0.8–1.0	0	4	0	4	0	0	0	0	0	0
Final Score		0.48	0.7	0.54	08.2	0.88	0.94	0.86	0.92	0.26	0.26

The inclusion of the BESS also enhances the SS index's performance, increasing its occurrence in higher ranges and thus allowing for a minimum self-sufficiency of 41% of the generated energy.

The BESS implementation reduced power exports to the grid regarding the PE index. Thus, the microgrid reduced the duration of violations between 21 and 40% (R2) from 6 to 3 years while increasing the duration below 20% (R1) to 7 years. Similarly, the PI index demonstrates that adopting the BESS also reduced violations in energy imports. Hence, violations of PI between 41 and 60% (R3) decrease to 1 year, while the duration in the range below 20% (R1) increases from 5 to 7 years.

Finally, regarding the GII index, the BESS did not contribute to reducing energy exchanges between the microgrid and the primary grid, maintaining the frequency distribution for the system without the storage system.

4.3.2. Impact on FCS Load Curves

The representative load curve profiles of FCS2 were generated using quantile representation, enabling analysis for different loading conditions. Quantile 1 (Q1) represents high load and low generation conditions, while quantile 0.5 (Q0.5) expresses average load and generation conditions, and quantile 0 (Q0) represents low load and high generation conditions [3].

Thus, FCS2 daily behavior for year 10 is presented based on the adopted conditions for the case study. It allows us to evaluate the microgrid performance and any potential negative impacts on the primary distribution grid, whether or not requiring infrastructure upgrades. For the first year, the behavior is illustrated in Figure 8.

By analyzing the FCS2 load profiles, it is observed that for Q1, the integration of the BESS allows reducing the maximum peak load of the daily period from approximately 121 kW to 111 kW, representing a reduction of 8.26%. Additionally, there is an average reduction in demand throughout the day of approximately 5%, contributing to a general decrease in energy imports, as was observed for the PI index.

For Q0.5, the BESS introduces energy autonomy for most of the day, reducing energy imports and the maximum peak demand by up to 10%. Therefore, under moderate load and generation conditions, the FCS can effectively manage generated energy for almost 60% of the day.

Considering Q0, the inclusion of the BESS in the FCS microgrid allows for a delay of power flow reversal in the primary grid for up to 6 h, maintaining a neutral load profile. However, in the subsequent hours, with the BESS SoC at 100%, the reverse power flow increases as per previous conditions.

Thus, analogous to the market share, in a scenario of 5% EV penetration, the FCS microgrid becomes autonomous from the primary grid for most of the day if load and generation conditions are not extreme.

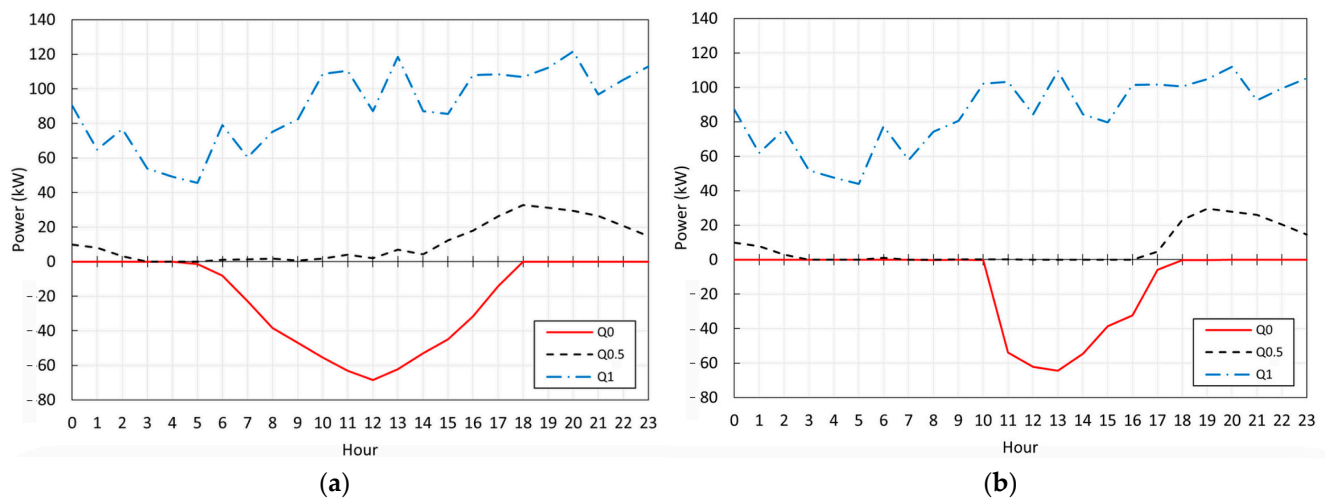


Figure 8. FCS2 load profiles for Year 10 (a) without BESS and (b) with BESS.

5. Conclusions

This paper presented a methodology for planning and analyzing microgrids for FCSs located on highways based on evaluating quantitative indexes to optimize the use of local energy resources and limit the impacts on the primary electrical grid. Through the concept of Nearly Zero Energy Buildings (NZEB), it was possible to relate the generation profile to local load demand (Load Matching) and the interaction between the microgrid and the main grid (Grid Interaction).

The methodology was applied to a study case that considered a portion of a highway in Brazil's southern region. For this purpose, a load model for FCSs was considered, incorporating accurate traffic data, EV characteristics, and a projection of EV market share over the next ten years in the country. Additionally, microgrid configurations (or Systems) were defined, and simulations of the resulting power flow with the primary grid were performed, allowing for a quantitative analysis of each System's performance using NZEB indicators. The annual model applied allowed the generation and load variations throughout the year, due to seasonality aspects and also the consideration of stochastic factors.

The analyses conducted enabled the identification of system characteristics that best fit the FCS's energy needs while presenting the best NZEB indexes over the study period. In other words, the methodology allows planning FCS microgrids, supporting decision-making to limit negative impacts on the main grid, sizing optimization, and reducing energy exchanges. This was possible by determining the PE, PI, and GII indexes, for example. Furthermore, the methodology allows a sensitivity analysis of the results to be carried out by varying the relevance weights of each indicator. It indicates the model's adaptation to the real conditions of each grid, adding robustness to the model.

The analyses were complemented by the characterization of representative profiles using quantiles, representing different load and generation conditions, thereby allowing for the temporal behavior of load at the FCS to be examined. It was found that the BESS promotes delay and reduction of the reversal peak power flow, further enhancing the considered indicators. In future work, it will be analyzed whether the gains obtained with the addition of BESS are interesting from a lamentation and operation costs point of view, comparing the solution with systems just with best-fit generation. This way, it is possible to measure the economic benefits of BESS inclusion.

Considering the need for public charging infrastructure to support the widespread adoption of EVs, particularly at FCSs located on highways, microgrids can reduce the high demands placed on these infrastructures from a grid point-of-view. However, local micro/mini generation systems, with or without storage, must be evaluated considering the trade-off between optimizing self-consumption and self-sufficiency and reducing impacts

on the primary electrical grid. Therefore, methodologies for the energy planning of these infrastructures, which are expected to grow in the coming years, should be considered, such as the one presented in this study.

Author Contributions: Conceptualization, M.S.d.C. and A.d.R.A.; Formal analysis, C.B.F.D., N.K.N. and L.N.F.d.S.; Methodology, M.S.d.C., C.B.F.D. and N.K.N.; Project administration, A.d.R.A.; Software, M.S.d.C. and C.B.F.D.; Supervision, L.N.F.d.S., N.K.N., and L.L.C.d.S.; Validation, L.L.C.d.S.; Writing—original draft, M.S.d.C.; Writing—review & editing, M.S.d.C., C.B.F.D., N.K.N., and L.N.F.d.S. All authors have read and agreed to the published version of the manuscript.

Funding: This research was funded by Electrical Energy State Company (CEEE-D) and Equatorial Energy Group (R&D project ANEEL-CEEE/EQUATORIAL/UFSM n° 5000004061), National Institute of Science and Technology on Distributed Generation Power Systems (INCT-GD), National Council for Scientific and Technological Development (CNPq—n° 405054/2022-0), Coordination for the Improvement of Higher Education Personnel—Brasil (CAPES—n° 23038.000776/2017-54), Foundation for Research of the State of Rio Grande do Sul (FAPERGS—n° 17/2551-0000517-1), and Federal University of Santa Maria (UFSM), Brazilian Institutes.

Data Availability Statement: The data presented in this study might be available on request from the corresponding author. The data are not publicly available due to confidentiality agreement with Equatorial Energia Group.

Conflicts of Interest: The authors declare no conflicts of interest.

References

- Delgado, F.; Costa, J.E.G.; Febraro, J.; da Silva, T.B. *Cadernos FGV Energia: Carros Elétricos*; FGV Energia: Rio de Janeiro, Brazil, 2017. Available online: https://fgvenergia.fgv.br/sites/fgvenergia.fgv.br/files/caderno_carros_eletricos-fgv-capa_ing_-_completo_-_rev2.pdf (accessed on 10 November 2024).
- EPE. *Eletromobilidade e Biocombustíveis*; Empresa de Pesquisa Energética. Ministério de Minas e Energia: Brasil, 2018. Available online: <https://www.epe.gov.br/sites-pt/publicacoes-dados-abertos/publicacoes/PublicacoesArquivos/publicacao-227/topico-457/Eletromobilidade%20e%20Biocombustiveis.pdf> (accessed on 10 November 2024).
- Das, H.S.; Rahman, M.M.; Li, S.; Tan, C.W. Electric vehicles standards, charging infrastructure, and impact on grid integration: A technological review. *Renew. Sustain. Energy Rev.* **2020**, *120*, 109618. [[CrossRef](#)]
- PNME. *1º Anuário Brasileiro da Mobilidade Elétrica*; Plataforma Nacional de Mobilidade Elétrica: Rio de Janeiro, Brazil, 2020.
- IEA. *Global EV Outlook 2021—Accelerating Ambitions Despite the Pandemic*; IEA: Paris, France, 2021.
- Da Costa, D. *Estações de Recarga Para Veículos Elétricos Alimentadas por Energia Solar Fotovoltaica: Estudo de Caso para Rodovia BR-381 Fernão Dias em 2030*; Universidade Federal de Itajubá: Itajubá, Brazil, 2021.
- ABVE. *Governo Anuncia Rota 2030 e Corta IPI Para Elétricos*; Associação Brasileira de Veículos Elétricos: São Paulo, Brazil, 2018.
- Hardman, S.; Jenn, A.; Tal, G.; Axsen, J.; Beard, G.; Daina, N.; Figenbaum, E.; Jakobsson, N.; Jochem, P.; Kinnear, N.; et al. A review of consumer preferences of and interactions with electric vehicle charging infrastructure. *Transp. Res. Part D Transp. Environ.* **2018**, *62*, 508–523. [[CrossRef](#)]
- Jochem, P.; Szimba, E.; Reuter-Oppermann, M. How many fast-charging stations do we need along European highways? *Transp. Res. Part D Transp. Environ.* **2019**, *73*, 120–129. [[CrossRef](#)]
- Da Silva, L.; Abaide, A.A.; Sausen, J.P.; Paixao, J.; Correa, C.H. Proposal of a load curve modeling applied to highway EV Fast charging stations. In Proceedings of the 2021 56th International Universities Power Engineering Conference (UPEC), Middlesbrough, UK, 31 August–3 September 2021; pp. 1–6.
- Kumar, J.; Parthasarathy, C.; Västi, M.; Laaksonen, H.; Shafie-Khah, M.; Kauhaniemi, K. Sizing and allocation of battery energy storage systems in Åland islands for large-scale integration of renewables and electric ferry charging stations. *Energies* **2020**, *13*, 317. [[CrossRef](#)]
- Alsaidan, I.; Khodaei, A.; Gao, W. A Comprehensive Battery Energy Storage Optimal Sizing Model for Microgrid Applications. *IEEE Trans. Power Syst.* **2018**, *33*, 3968–3980. [[CrossRef](#)]
- da Silveira, A.S. *Método Heurístico para Otimização do Dimensionamento de uma Microrrede de Energia*; Universidade Federal de Santa Maria: Santa Maria, Brazil, 2021.
- Yoldaş, Y.; Önen, A.; Muyeen, S.M.; Vasilakos, A.V.; Alan, İ. Enhancing smart grid with microgrids: Challenges and opportunities. *Renew. Sustain. Energy Rev.* **2017**, *72*, 205–214. [[CrossRef](#)]
- Silva, L.N.F.d.; Capeletti, M.B.; Abaide, A.d.R.; Pfitscher, L.L. A Stochastic Methodology for EV Fast-Charging Load Curve Estimation Considering the Highway Traffic and User Behavior. *Energies* **2024**, *17*, 1764. [[CrossRef](#)]
- Luthander, R.; Widén, J.; Nilsson, D.; Palm, J. Photovoltaic self-consumption in buildings: A review. *Appl. Energy* **2015**, *142*, 80–94. [[CrossRef](#)]

17. Raghavan, A.K. PV Enabled Net Zero EV Charging Station: System Design and Simulation Studies. Master's Thesis, University of Waterloo, Waterloo, ON, Canada, 2018.
18. Salom, J.; Marszal, A.; Candanedo, J.; Widén, J.; Lindberg, K.B.; Sartori, I. Analysis of Load Match and Grid Interaction Indicators in NZEB with High-Resolution Data. 2014. Available online: https://upcommons.upc.edu/bitstream/handle/2117/77544/T4_0A52--LMGI-in-Net-ZEBs--STA-Technical-Report.pdf (accessed on 10 November 2024).
19. Berggren, B.; Widen, J.; Karlsson, B.; Wall, M. Evaluation and optimization of a swedish net zebusing load matching and grid interaction indicators. In Proceedings of the First Building Simulation and Optimization Conference BSO-2012, Loughborough, UK, 10–11 September 2012; pp. 285–292.
20. Presidência da República, “Lei 14.300/2022. Diário Oficial da União: Brasil. 2022. Available online: <https://legis.senado.leg.br/norma/35420157/publicacao/35420471> (accessed on 10 November 2024).
21. Grisales-Noreña, L.F.; Restrepo-Cuestas, B.J.; Cortés-Cacedo, B.; Montano, J.; Rosales-Muñoz, A.A.; Rivera, M. Optimal Location and Sizing of Distributed Generators and Energy Storage Systems in Microgrids: A Review. *Energies* **2023**, *16*, 106. [CrossRef]
22. Mowry, A.M.; Mallapragada, D.S. Grid impacts of highway electric vehicle charging and role for mitigation via energy storage. *Energy Policy* **2021**, *157*, 112508. [CrossRef]
23. Muttaqi, K.M.; Isac, E.; Mandal, A.; Sutanto, D.; Akter, S. Fast and random charging of electric vehicles and its impacts: State-of-the-art technologies and case studies. *Electr. Power Syst. Res.* **2024**, *226*, 109899. [CrossRef]
24. Nandini, K.K.; Jayalakshmi, N.S.; Jadoun, V.K. A combined approach to evaluate power quality and grid dependency by solar photovoltaic based electric vehicle charging station using hybrid optimization. *J. Energy Storage* **2024**, *84*, 110967.
25. Azimi, M.; Al-shibli, W.K.; Zand, M. Charging management of electric vehicles with the presence of renewable resources. *Renew. Energy Focus* **2024**, *48*, 100536.
26. Shafiei, M.; Ghasemi-Marzbali, A. Electric vehicle fast charging station design by considering probabilistic model of renewable energy source and demand response. *Energy* **2023**, *267*, 126545. [CrossRef]
27. Khaksari, A.; Tsaousoglou, G.; Makris, P.; Steriotis, K.; Efthymiopoulos, N.; Varvarigos, E. Sizing of electric vehicle charging stations with smart charging capabilities and quality of service requirements. *Sustain. Cities Soc.* **2021**, *70*, 102872. [CrossRef]
28. Ahmad, F.; Iqbal, A.; Ashraf, I.; Marzband, M.; Khan, I. Optimal Siting and Sizing Approach of Plug-in Electric Vehicle Fast Charging Station using a Novel Meta-heuristic Algorithm. In Proceedings of the 2022 2nd International Conference on Emerging Frontiers in Electrical and Electronic Technologies (ICEFEET), Patna, India, 24–25 June 2022; pp. 1–6.
29. Kong, W.; Luo, Y.; Feng, G.; Li, K.; Peng, H. Optimal location planning method of fast charging station for electric vehicles considering operators, drivers, vehicles, traffic flow and power grid. *Energy* **2019**, *186*, 115826. [CrossRef]
30. Sun, B. A multi-objective optimization model for fast electric vehicle charging stations with wind, PV power and energy storage. *J. Clean. Prod.* **2021**, *288*, 125564. [CrossRef]
31. Ebrahimi, J.; Abedini, M.; Rezaei, M.M.; Nasri, M. Optimum design of a multi-form energy in the presence of electric vehicle charging station and renewable resources considering uncertainty. *Sustain. Energy Grids Netw.* **2020**, *23*, 100375. [CrossRef]
32. Keramati, F.; Mohammadi, H.R.; Shiran, G.R. Determining optimal location and size of PEV fast-charging stations in coupled transportation and power distribution networks considering power loss and traffic congestion. *Sustain. Energy Grids Netw.* **2024**, *38*, 101268. [CrossRef]
33. Amir, M.; Zaheeruddin; Haque, A.; Bakhsh, F.I.; Kurukuru, V.S.B.; Sedighizadeh, M. Intelligent energy management scheme-based coordinated control for reducing peak load in grid-connected photovoltaic-powered electric vehicle charging stations. *IET Gener. Transm. Distrib.* **2023**, *18*, 1205–1222. [CrossRef]
34. Jaysawal, R.K.; Chakraborty, S.; Elangovan, D.; Padmanaban, S. Concept of net zero energy buildings (NZEB)—A literature review. *Clean. Eng. Technol.* **2022**, *11*, 100582. [CrossRef]
35. Galisai, S.; Ghiani, E.; Pilo, F. Multi-Objective and Multi-Criteria Optimization of Microgrids for Nearly Zero-Energy Buildings. In Proceedings of the SEST 2019-2nd International Conference on Smart Energy Systems and Technologies, Porto, Portugal, 9–11 September 2019; pp. 1–6.
36. Salom, J.; Widén, J.; Candanedo, J.; Sartori, I.; Voss, K.; Marszal, A. Understanding net zero energy buildings: Evaluation of load matching and grid interaction indicators. In Proceedings of the Building Simulation 2011: 12th Conference of International Building Performance Simulation Association, Sydney, Australia, 14–16 November 2011; Volume 6, pp. 2514–2521.
37. Ferraro, M.; Sergi, F.; Antonucci, V.; Guarino, F.; Tumminia, G.; Cellura, M. Load match and grid interaction optimization of a net zero energy building through electricity storage: An Italian case-study. In Proceedings of the International Conference on Environment and Electrical Engineering, IEEEIC 2016, Florence, Italy, 7–10 June 2016; pp. 1–5.
38. Stamatellos, G.; Stamatellou, A.M. The Interaction between Short- and Long-Term Energy Storage in an nZEB Office Building. *Energies* **2024**, *17*, 1441. [CrossRef]
39. Alfieri, S.; Piccini, S.; Kermani, M. Feasibility study of Nearly Zero Energy Building in a real Microgrid case study. In Proceedings of the Proceedings-2019 IEEE International Conference on Environment and Electrical Engineering and 2019 IEEE Industrial and Commercial Power Systems Europe, IEEEIC/I and CPS Europe 2019, Genova, Italy, 11–14 June 2019.
40. Attia, S.; Kurnitski, J.; Kosiński, P.; Borodinecs, A.; Belafi, Z.D.; István, K.; Krstić, H.; Moldovan, M.; Visa, I.; Mihailov, N.; et al. Overview and future challenges of nearly zero-energy building (nZEB) design in Eastern Europe. *Energy Build.* **2022**, *267*, 112165. [CrossRef]

41. Dávi, G.A.; Castillo-Cagigal, M.; Caamaño-Martín, E.; Solano, J. Evaluation of Load Matching and Grid Interaction Indexes of a Net Plus-Energy House in Brazil with a Hybrid PV System and Demand-Side Management. In Proceedings of the 32nd European Photovoltaic Solar Energy Conference and Exhibition, Munich, Germany, 20–24 June 2016; pp. 2692–2698.
42. Lambert, T.; Gilman, P.; Lilienthal, P. Micropower System Modeling with Homer. In *Integration of Alternative Sources of Energy*; John Wiley & Sons, Inc.: Hoboken, NJ, USA, 2006; pp. 379–418.
43. NASA. Prediction of Worldwide Energy Resource (POWER) 2022. [Online]. Available online: <https://power.larc.nasa.gov/> (accessed on 12 December 2024).
44. Lilienthal, P.D.; Lambert, T.W.; Gilman, P. Computer Modeling of Renewable Power Systems. In *Encyclopedia of Energy*; Cleveland, C.J., Ed.; Elsevier Inc.: Amsterdam, The Netherlands, 2004; pp. 633–647.
45. Shahinzadeh, H.; Moazzami, M.; Fathi, S.H.; Gharehpetian, G.B. Optimal sizing and energy management of a grid-connected microgrid using HOMER software. In Proceedings of the 2016 Smart Grids Conference, SGC 2016, Kerman, Iran, 20–21 December 2016; pp. 13–18.
46. Lucca, T.G.; Darui, C.; Silva, L.; Abaide, A.; Neto, N.K.; da Cruz, M. Optimized allocation of fast charging stations in highways involving multiple criteria. In Proceedings of the CIRED Porto Workshop 2022: E-Mobility and Power Distribution Systems, Porto, Portugal, 2–3 June 2022; pp. 2–3.
47. DNIT. *PNCT—Plano Nacional de Contagem de Tráfego*; Departamento Nacional de Infraestrutura de Transportes: Brasil, 2022. Available online: <https://www.gov.br/dnit/pt-br/assuntos/planejamento-e-pesquisa/planejamento/contagem-de-trafego> (accessed on 10 November 2024).

Disclaimer/Publisher’s Note: The statements, opinions and data contained in all publications are solely those of the individual author(s) and contributor(s) and not of MDPI and/or the editor(s). MDPI and/or the editor(s) disclaim responsibility for any injury to people or property resulting from any ideas, methods, instructions or products referred to in the content.